HHS Public Access

Author manuscript

Circ Res. Author manuscript; available in PMC 2024 November 10.

Published in final edited form as:

Circ Res. 2023 November 10; 133(11): 885–898. doi:10.1161/CIRCRESAHA.123.323119.

Myeloid Cell Derived IL1β Contributes to Pulmonary Hypertension in HFpEF

Vineet Agrawal, MD, PhD[1,2], **Jonathan A. Kropski, MD**[3], **Jason J. Gokey, PhD**[3], **Elizabeth Kobeck, BS**[1], **Matthew B. Murphy, PharmD, PhD**[4], **Katherine T. Murray, MD**[1,4], **Niki L. Fortune**[2], **Christy S. Moore, BS**[3], **David F. Meoli, MD, PhD**[1,2], **Ken Monahan, MD**[1], **Yan Ru Su, MD**[1], **Thomas Blackwell, BS**[3], **Deepak K. Gupta, MD, MSc**[1], **Megha H. Talati, PhD**[3], **Santhi Gladson, MS**[3], **Erica J. Carrier, PhD**[3], **James D. West, PhD**[3], **Anna R. Hemnes, MD**[3]

[1]Division of Cardiovascular Medicine, Department of Medicine, Vanderbilt University Medical Center, Nashville, TN

[2]Tennessee Valley Healthcare System Nashville Veteran Affairs Hospital, Nashville, TN

[3]Division of Pulmonary, Allergy, and Critical Care, Department of Medicine, Vanderbilt University Medical Center, Nashville, TN

[4]Division of Clinical Pharmacology, Department of Medicine, Vanderbilt University Medical Center, Nashville, TN

Abstract

Background: Pulmonary hypertension (PH) in heart failure with preserved ejection fraction (HFpEF) is a common and highly morbid syndrome, but mechanisms driving PH-HFpEF are poorly understood. We sought to determine whether a well-accepted murine model of HFpEF also displays features of PH, and we sought to identify pathways that might drive early remodeling of the pulmonary vasculature in HFpEF. .

Methods: Eight-week-old male and female C57BL/6J mice received either L-NAME and high fat diet (HFD) or control water and diet for 2, 5, and 12 weeks. Db/db mice were studied as a second model of HFpEF. Early pathways regulating PH were identified by bulk and single cell RNA sequencing. Findings were confirmed by immunostain in lungs of mice or lung slides from clinically performed autopsies of PH-HFpEF patients. ELISA was used to verify IL1β in mouse lung, mouse plasma, and also human plasma from PH-HFpEF patients obtained at the time of right heart catheterization. Clodronate liposomes and an anti-IL1β antibody were utilized to deplete macrophages and IL1β, respectively, to assess their impact on pulmonary vascular remodeling in HFpEF in mouse models.

Send Correspondence to: Vineet Agrawal, MD, PhD, Nashville Veterans Affairs Medical Center, 1310 24th Avenue South, ACRE Building, F-305, Nashville, TN, 37212, vineet.agrawal@vumc.org.

Author contributions: Conception/Design of study (VA, ARH); Data acquisition, analysis, and interpretation (VA, JAK, JJG, EK, MBM, KTM, NLF, CSM, DFM, KM, YRS, TB, DKG, MHT, SG, JDW, ARH); Manuscript preparation (VA, JDW, ARH); Final approval of work and manuscript (VA, JAK, JJG, EK, MBM, KTM, NLF, CSM, DFM, KM, YRS, TB, DKG, MHT, SG, JDW, ARH)

DISCLOSURES

All authors report no disclosures relevant to the topic of the manuscript.

Results: L-NAME/HFD treated mice developed PH, small vessel muscularization, and right heart dysfunction. Inflammation-related gene ontologies were over-represented in bulk RNA sequencing analysis of whole lungs, with an increase in $CD68^{+}$ cells in both murine and human PH-HFpEF lungs. Cytokine profiling showed an increase in IL1β in mouse and human plasma. Finally, clodronate liposome treatment in mice prevented PH in L-NAME/HFD treated mice, and IL1β depletion also attenuated PH in L-NAME/HFD treated mice.

Conclusions: We report a novel model for the study of PH and right heart remodeling in HFpEF, and we identify myeloid cell derived IL1β as an important contributor to PH in HFpEF.

Graphical Abstract

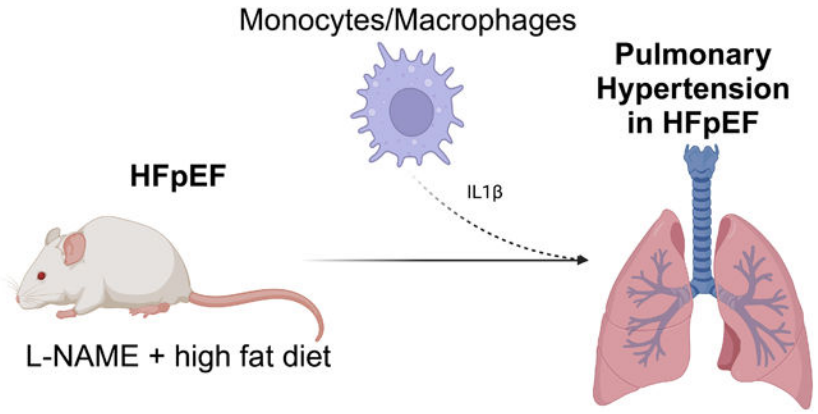

Keywords

Animal Models of Human Disease; Inflammation; Pulmonary Biology

INTRODUCTION

Pulmonary hypertension (PH) is a heterogenous syndrome defined by invasively measured mean pulmonary arterial pressure > 20 mmHg. The most common worldwide cause of PH is left heart failure, and patients with heart failure with preserved ejection fraction and pulmonary hypertension (PH-HFpEF) carry the worst prognosis.[1] Despite studies demonstrating similar degrees of vascular remodeling between patients with PH-HFpEF and other conditions such as pulmonary arterial hypertension (PAH),[2] the pathogenesis of PH-HFpEF is largely unknown, precluding the development of therapies that could improve morbidity and mortality in PH-HFpEF. A key limiting factor in advancing our understanding of the pathogenesis underlying PH-HFpEF has been the paucity of animal models that faithfully recapitulate human features of the disease.[3] Models of HFpEF with concomitant PH have been reported in large animals and rodents, but relatively few murine models of HFpEF have been described that mimic features of pulmonary vascular remodeling seen in patients.[3,4]

Schiattarella *et al* previously reported a now widely accepted murine model of HFpEF that uses a combination of high fat diet (HFD) and N(gamma)-nitro-L-arginine methyl ester (L-NAME) to recapitulate many of the cardiac and extra-cardiac features of HFpEF.[5] However,

whether this model recapitulates the pulmonary vascular remodeling phenotype commonly seen in human HFpEF is now known.[4,6] Our study hypothesized that L-NAME and HFD would also result in pathologic pulmonary vascular remodeling, and we further sought to identify early pathways that might regulate this process. Our data show that myeloid derived IL1β is an important mediator of PH in HFpEF, which we also corroborated in human lung slides from autopsies of PH-HFpEF patients and plasma samples from PH-HFpEF patients.

METHODS

Data Availability

All animal data are available upon reasonable request to the corresponding author. Bulk and single cell sequencing raw genomic data are available through the Gene Expression Omnibus (GEO) database at NCBI (GSE244304, GSE244309). Code used for scRNA-seq analysis and figure generation will be available at https://github.com/kropskilab/myeloid_il1b.

All animal studies were approved by the Vanderbilt University Institutional Animal Care and Use Committee (IACUC). Collection of human plasma samples and tissue sections from human autopsies was approved by the Institutional Review Board at Vanderbilt University Medical Center. Male and female C57BL/6J mice were purchased at 8 weeks of age from Jackson Laboratories (Bar Harbor, ME, USA). Male and female db/db mice were purchased from Jackson Laboratories at the age of 16 weeks of age (Bar Harbor, ME, USA). No animals were excluded from the study. Mice were randomized by even/odd number into each experimental group after direct purchase. Scientists were not blinded to the experimental group for each mouse.

Animal Studies

To induce the HFpEF phenotype, C57BL/6J mice at 8 weeks of age (Jackson Laboratories, Bar Harbor, ME) were administrated L-NAME in sterile water (0.5 g/L) (pH 7.0) and given a 60% lipid content HFD *ad libitum* for 2, 5, or 12 weeks (BioServ, Flemington, NJ, USA). Control mice received regular water with a calorie neutral 6% lipid content low fat diet (BioServ, Flemington, NJ). At each time point, mice underwent anesthetized echocardiography, open chest catheterization, and tissue harvest as previously described with no deviations.[6] Structural analysis of lung tissue included a hematoxylin and eosin stain as well as an immunostain for muscularization of vessels as previously described with no deviations.[7] Plasma was collected at the time of catheterization by direct puncture of the heart and withdrawal of up to 1 ml of blood in a EDTA containing tube, which was then centrifuged at 1500 g x 15 minutes at 4 °C. Lung lysate was obtained after removing lungs and homogenizing in RIPA buffer using a bead mill. Cytokine levels were measured by pooling plasma and lung lysate from 5 mice treated with either L-NAME/HFD or control water/diet for 5 weeks and were assayed using an antibody-based cytokine array (R&D Systems, ARY006) according to the manufacturer's instructions. Mouse IL1β in plasma was measured by ELISA (Thermo, BMS6002) following manufacturer's instructions.

Mouse Echocardiography and Catheterization

Mouse echocardiography and catheterization was performed as previously reported.[6] One day prior to catheterization, mice were anesthetized with 2–3% isoflurane. Depilatory cream was applied to the thorax. Mice were then placed on a heated table in supine position and images were acquired using the VisualSonics Vevo700 Platform and 707B transducer (30 MHz) in B-mode, M-mode, and Doppler mode. Parasternal long-axis, short-axis, and modified RV-centric views were obtained as previously described.[7] Thereafter, mice were allowed to recover for 24 hours before undergoing anesthesia again with 2–3% isoflurane for open chest catheterization. Mice were orotracheally intubated with 22g catheter, mechanically ventilated at 18 cc/kg, and anesthetized with 2–3% vaporized isoflurane general anesthesia. On a heated surgical table in supine, ventral side-up position, a vertical incision was made along the linea alba in the rectus abdominus sheath with scissors and cautery, and extended laterally. Cautery was then used to take down the diaphragm and exposure the thorax. A 1.4 French Mikro-tip catheter was directly inserted into the left ventricle for measurement of pressure and volume within the left ventricle. Afterwards, the catheter was removed and directly inserted into the right ventricle. Hemostasis of the left ventricle was ensured prior to catheterization of the right ventricle to ensure no effect of volume loss on findings. Hemodynamics were continuously recorded with a Millar MPVS-300 unit coupled to a Powerlab 8-SP analog-to-digital converter acquired at 1000 Hz and captured to a Macintosh G4 (Millar Instruments, Houston, TX). Thereafter, direct cardiac puncture was used to phlebotomize mice using a heparinized syringe and mice were sacrificed with cervical dislocation. Tissue and samples were then harvested for downstream studies from mice, including morphometric measurements. Volume was measured in relative volume units based on recommended calibrations from Millar Instruments. Pulmonary vascular resistance was calculated in Wood units using the transpulmonary gradient to cardiac output ratio, as measured by catheterization.

Plasma Sample Collection from Patients

Samples were analyzed from a previous prospective, cross-sectional study.[8,9] The study was approved by the Vanderbilt University Institutional Review Board and all participants provided written informed consent. Inclusion criteria included patients aged 18 or older, referral for right heart catheterization with or without concomitant left heart catheterization as part of their usual care. Exclusion criteria included LVEF ≤ 40%, atrial fibrillation on the day of catheterization, significant anemia (hemoglobin < 10 g/dL and hematocrit < 30%), pregnancy, and treatment with PAH-specific medications or nitrates. Samples were collected after Swan-Ganz catheter placement in the proximal pulmonary artery or wedge position, confirmed by pressure waveform analysis. A 5–10 cc blood sample was collected with minimal aspiration pressure, immediately placed on ice, and then hand-delivered to the Vanderbilt Core Laboratory for Cardiovascular Translational and Clinical Research where plasma was separated, aliquoted, and stored in a −80 °C freezer for analysis.
For classification of cases, all hemodynamic tracings were independently reviewed by cardiologists (DFM and KM), and the following definitions were used for classification: (1) PH-HFpEF: mPAP ≥ 20 mmHg and pulmonary artery wedge pressure > 15 mmHg) vs o(2) no PH (mPAP < 20 mmHg). All pressures were measured at end expiration at rest in supine patients. Biomarker analysis for IL1β was conducted following manufacturer's

recommended protocol on samples (Thermo, A35574, Waltham, MA) in triplicate on each sample.

Lung Autopsy Slide Analysis

To identify clinically conducted autopsies in patients with pulmonary hypertension and heart failure, we interrogated Vanderbilt University Medical Center's clinical autopsy database. Autopsy cases between 2013 and 2018 were initially screen for the presence of terms "heart failure" in the case synopsis or pathology report with additional filters of patient aged 18 or older. Cases were then individually reviewed (VA). Inclusion criteria included any pre-mortem right heart catheterization performed that demonstrated mean PA pressure > 20 mmHg and pulmonary arterial wedge pressure > 15 mmHg as well as echocardiography-based on cardiac MRI-based measurement of left ventricular ejection fraction ≥ 50%. Pre-determined exclusion criteria included: (1) known pre-existing lung disease such as obstructive lung disease as this would alter lung histology, (2) the presence of a primary pulmonary vascular disease such as pulmonary arterial hypertension or pulmonary veno-occlusive disease, (3) cause of death that was deemed to be due to acute lung injury (ARDS) or infection (pneumonia), (4) presence of congenital heart disease, and (4) presence of an autoimmune condition or immunosuppressive therapy for any indication as this may alter vascular remodeling via alteration of inflammatory pathways. A total of 231 autopsy cases were reviewed, of which 20 met inclusion criteria for PH and HFpEF without any exclusion criteria. Of those, 8 still had available blocks of lung tissue, which were used for the final analysis. An additional 8 lung tissue sections were randomly chosen among excluded autopsies of patients without heart failure.

Western Blot and Immunostaining

Lung slides, both mouse and human, were originally sectioned into 5 μm sections and 2 consecutively cut sections placed on each slide. Mouse lungs were inflated with low melting point agarose were deparaffinized and underwent heat antigen retrieval for 20 min in Tris EDTA pH 9 antigen retrieval buffer. Samples were blocked for 2 h in 10% goat serum and 1% bovine serum albumin (BSA) prior to incubation in primary antibody overnight in 0.5% BSA. They were then incubated in secondary antibody diluted in phosphate buffered saline prior to mounting with Vectashield 4',6-diamidino-2-phenylindole DAPI (Vector Laboratories, Burlingame, CA). Images were then taken on the Nikon Eclipse Ti confocal microscope (Nikon USA, Melville, NY). Primary antibody used was CD68 (Invitrogen, MA5–13324) at 1:100 concentration. Secondary antibody was used at 1:250 concentration (Donkey anti-rabbit (A-21202) or anti-mouse (A-21206) Alexa Fluor 488; Goat anti-rabbit (A-11012) or anti-mouse (A-11005) Alexa Fluor 594; Thermo Fisher Scientific). For the second section on each slide, the primary antibody was omitted to distinguish non-specific secondary antibody staining from genuine target staining.

For Western blots, tissue was homogenized in RIPA buffer containing protease and phosphatase inhibitors. Protein was quantified by BCA assay, heated at 99 °C for 7 min to denature protein, and then run on a 4–12% Bis-Tris gel and transferred on to PVDF by wet transfer. Thereafter, samples were blocked with 5% bovine serum albumin in TBS-T, incubated in primary antibody at 1:1000 concentration overnight in blocking buffer, and then

incubated with 1:5000 concentration of HRP-conjugated secondary antibody in 5% milk in TBS-T. After washing and incubation in chemiluminescent substrate, blots were imaged on an iBright 1500 imager (Thermo Scientific). Blots were quantified using ImageJ. Primary antibodies used included IL1β (Cell Signal, D6D6T, 31202) and CD68 (Invitrogen, MA5–13324).

Monocyte/Macrophage and IL1β Depletion Studies

To deplete circulating monocytes and phagocytic cells, C57BL/6J mice were given twice weekly intraperitoneal injections of 100 μl of 5 mg/ml of either clodronate liposomes or phosphate buffered containing liposomes (Liposoma, Amsterdam, Netherlands; Batch Nos: C29E0622, P20E0522). Mice were concurrently treated with either L-NAME/HFD or control water/diet, as outlined above, for 5 weeks. To deplete macrophages more selectively, C57BL/6J mice were treated with L-NAME/HFD or control water/diet for 3 weeks, followed by 2 weeks of twice weekly intraperitoneal injections of 100 μg of anti-F4/80 antibody (BE0206, BioXCell, Lebanon, NH) or isotype control (BE0090, BioXCell, Lebanon, NH). To deplete IL1β, C57BL/6J mice were treated with L-NAME/HFD or control water/diet for 3 weeks. During weeks 4 and 5, they were given twice weekly intraperitoneal injections of 100 μg of either an anti-IL1β (BE0246, BioXCell, Lebanon, NH) or an isotype control antibody (BE0091, BioXCell, Lebanon, NH). Treatment in the final two weeks was chosen in all antibody treatments to prevent the development of potentially confounding autoantibodies to the treatment.

Bulk RNA Sequencing

Whole lung was flash frozen after treating C57BL/6J mice with either 5 weeks of either L-NAME/HFD or control water/diet. RNA was isolated using the RNeasy kit (Qiagen) and submitted to Novogene (Sacramento, CA) for paired end 150 sequencing on an Illumina platform. A nominal read depth of 30 million RNA (60 million ends) per animal was used. These were uploaded to and analyzed on the Partek platform, using the STAR aligner to align to the mm39 reference mouse genome. An average of 96% of reads aligned to genome (94%−97%). Counts were normalized to Counts Per Million.

Single cell RNA-sequencing

Mouse lungs were cleared of red blood cells by cardiac perfusion with 3 mL of sterile saline before excision and placement into a C-Tube (Miltenyi) (one C-tube/mouse) containing 5 mL lung digest solution (5 mL phenol free DMEM (Gibco), Dispase (Roche 04942078001), collagenase (Sigma-Aldrich C0130–1G), and 5uL DNAse (10,000iU)). Lungs were dissociated using a gentleMacs dissociator for 17 min at 37 degrees Celsius. Cell suspensions were passed through 100 μm then 70 μm cell strainers and washed 3 times in 5 mL cell buffer (phenol free DMEM, 0.2 mM EDTA, and 0.5% FBS). Cells were centrifuged at 500 g for 10 min. Red blood cells were removed by lysing with 2 mL ACK buffer (KD Medical RGC-3015) for 5 min. Cells were then washed, centrifuged, passed through a 40 μm cell strainer and resuspended for counting. Cell-hashing was performed by incubating $1X10^6$ cells with Total-SeqB (B0301-B0304) cell-hashing antibodies (Biolegend) for 30 min. Cells were then washed 3 times in cell buffer, and equal numbers of cells from each of the 4 mice per condition were pooled into a single reaction for scRNA-seq library

generation using the 10X Genomics Chromium 3'v3 kit. Library sequencing was performed on an Illumina Novaseq6000 targeting 50,000 reads per cell.

scRNA-seq analysis

Alignment and demultiplexing were performed using CellRanger v7.0.1. Ambient RNA filtering was performed using CellBender v0.2.2.[10] ScRNA-seq analysis was performed using Seurat[11] v5 adapted from our previous work[12–14] with additional data visualization using scCustomize (https://doi.org/10.5281/zenodo.7534950). Demultiplexing was performed using the HTOdemux function, and singlet cells were carried forward for downstream analysis. Following quality-control filtering (excluding cells with < 500 or > 5000 genes, and cells with > 10% mitochondrial reads), data were normalized and scaled using the SCTransform function, including mitochondrial and ribosomal percentages as regression variables, followed by principal components analysis, neighborhood graph calculation and UMAP embedding using 45 dimensions, and recursive louvain-clustering/ subclustering. Heterotypic doublet clusters were identified by co-expression of lineage-specific marker genes, and cell annotation was performed manually, informed by published reference datasets.[15,16] Cell-type specific differential expression was performed on SCT-transformed counts using the Wilcoxon test. Gene ontology enrichment analysis was performed using PANTHER.

Statistical Methods

Based on prior studies, we aimed to identify a 20% change in outcomes (primary outcome of RV systolic pressure) with underlying 15% variance in measurements between mice. With $\alpha = 0.05$, and $\beta = 0.2$, we expected a sample size of 8 mice per group to be adequate to detect differences between groups. Physiologic findings from animal studies are presented as mean ± standard error (SEM). Data were analyzed in GraphPad Prism using non-parametric Mann Whitney test, Kruskal Wallis test, or Fisher's exact test.Group differences in bulk RNA sequencing data were assessed using Kruskal-Wallis test, and gene ontology determined using Webgestalt (webgestalt.org). In single cell sequencing analysis, cell-type specific differential expression was performed on SCT-transformed counts using the Wilcoxon test. Gene ontology enrichment analysis was performed using PANTHER. We tested for sex differences for all results in our study and did not detect any significant sex-based differences.

RESULTS

L-NAME and High Fat Diet Cause Pulmonary Vascular Remodeling with RV Dysfunction

Mice exposed to L-NAME/HFD demonstrated features of human HFpEF including preserved cardiac output and left ventricular ejection fraction, increased systemic blood pressure and left atrial diameter, as well as weight gain (Suppl Figs 1,2). Moreover, as early as 2 weeks of L-NAME/HFD exposure, these mice manifest PH as increased pulmonary vascular resistance, right ventricular systolic pressure, right ventricular mass (Fig 1A–C) with histologic evidence for pulmonary vascular remodeling with increased muscularization of small vessels (< 50 μm) (Fig 1D) and medial wall thickness (Fig 1E). Despite a normal stroke volume (Fig 2A), mice exposed to L-NAME/HFD demonstrated an

increase in right ventricular relaxation time constant τ (Fig 2B), decrease in end-systolic to end-arterial elastance ratio (Ees/Ea) (Fig 2C), increase in liver weight as a marker of right ventricular congestion (Fig 2D), and an increase in right ventricular end-diastolic pressure (Fig 2E). These findings were all suggestive of a load-stressed right ventricle with features of decompensation.

L-NAME/HFD Treatment Results in Increased CD68$^+$ Cells in Lungs

We next sought to better understand pathways that might contribute to pulmonary vascular remodeling after treatment with L-NAME and HFD. Bulk RNA sequencing was performed after 5 weeks of treatment to identify transcripts and gene ontologies over-represented in mice receiving L-NAME/HFD compared to controls. In L-NAME/HFD-treated lungs, the top 15 over-represented gene ontologies all represented pathways related to inflammation or immunity (Fig 3A, Table S1). Supporting these findings, many of the top transcripts that were differentially expressed included transcripts for cytokines such as Ccr7, Ccl5, Il12a, and Cxcl14 (Fig 3B), all known chemokines that affect macrophage polarization and recruitment. To better understand cell types that might be contributing to these changes, we used RNA sequencing to probe transcript level expression of putative markers for T cells, B cells, monocyte/macrophages, and dendritic cells. Only CD68, a marker of macrophages, was significantly increased (Fig 3C), although a positive trend for expression was observed for other cell markers. Increased CD68 expression was confirmed in lungs by Western blot (Suppl Fig 3). We also found an increase in the number of CD68$^+$ cells in lungs of L-NAME/HFD treated mice (Fig 3D) as well as in a second animal model of HFpEF (db/db mice). Additional studies confirmed that the db/db mice, which spontaneously develop HFpEF, also develop pulmonary hypertension (Suppl Fig 4). Finally, CD68$^+$ cells were elevated in the lungs sections of patients with hemodynamically confirmed PH-HFpEF who clinically underwent autopsies (Fig 3E, Suppl Fig 5, Table S2).

L-NAME/HFD Treatment Results in Increased IL1β in Lungs

We next investigated whether L-NAME and high fat diet treatment affects the local and circulating cytokine proteome. By cytokine array, an increase in protein expression of a number of cytokines such as CCL5 and IL1β was detected in the lung lysate, but not in the plasma, of L-NAME/HFD treated mice (Fig 4A, Suppl Fig. 6). Given known effects of IL1β on vascular function,[17] we next focused our analysis on IL1β in PH-HFpEF. We confirmed an increase in protein expression of IL1β in the lungs of L-NAME/HFD-treated mice by Western blot (Fig 4B) and ELISA (Fig 4C). Finally, we confirmed in collected plasma from patients undergoing clinically indicated right heart catheterization an increase in circulating IL1β levels in venous blood, pulmonary arterial blood, and pulmonary capillary wedge blood of HFpEF patients with PH compared to non-PH controls (Fig 4D).

Monocyte/Macrophage Populations Display Pro-inflammatory Phenotype and Express IL1β

To investigate the phenotype of the monocyte/macrophage populations as well as cellular sources of IL1β in the lungs of L-NAME/HFD-treated mice, single cell RNA sequencing was performed. We identified 30 distinct cell populations within the lungs (Fig 5A–B, Suppl Fig. 6) with similar UMAP profiles for both L-NAME/HFD- and control water/diet-treated mice (Fig. 5B). There were proportional increases in numbers of inflammatory

cells in L-NAME/HFD treated mouse lungs including B-cell, T-cell, monocyte/macrophage, NK cell, and neutrophil populations (Suppl Fig. 6). The transcriptional phenotype of monocyte, monocyte-dendritic cell, monocyte-derived macrophage, and activated monocyte populations more closely resembled that of pro-inflammatory M1-like macrophages (Fig 5C), with directionally similar transcript expression changes by bulk RNA sequencing in whole lung (Suppl Fig. 7). On the other hand, alveolar macrophage populations predominantly demonstrated a decrease in M1-associated transcripts and an increase in M2-associated transcripts (Fig 5C). Nearly 90% of monocytes and 40% of activated monocyte, dendritic cells, and monocyte dendritic cells identified were Ccr2+, a marker of circulating monocyte/macrophage populations (Fig. 5D). Expression of IL1β transcripts was identified predominantly in neutrophil, activated monocyte, monocyte, and monocyte-derived macrophage populations (Fig 5D). The selective expression of IL1β in myeloid cell populations in the lung is congruent with published single cell RNA sequencing atlases of human lung in other disease processes such as idiopathic pulmonary fibrosis as well (ipfcellatlas.com)

Myeloid Cells Contribute to Pulmonary Vascular Remodeling in HFpEF

We next sought to test the hypothesis that circulating monocyte/macrophage populations contribute to pulmonary vascular remodeling in our L-NAME/HFD model of PH-HFpEF. To deplete circulating monocytes and macrophages, mice were treated with L-NAME/HFD for 5 weeks while receiving twice weekly injections of clodronate or PBS containing liposomes (Fig 6A). Clodronate treatment resulted in reduced CD68 expression in mouse lungs (Fig 6B) as well as lower IL1β levels by ELISA (Fig 6C). Mice treated with clodronate compared to PBS liposomes also demonstrated less weight gain, near normal RV systolic pressure, normal RV mass compared to LV and septal mass in the heart, near normal RV end-diastolic pressure, and a decrease in muscularization of small vessels histologically in the lungs (Fig 6D,E). Taken together, these data indicate that a circulating population of myeloid cells are recruited to the lung and contribute to pathologic pulmonary vascular remodeling and pulmonary hypertension in the L-NAME/HFD model of HFpEF. Since clodronate can potentially deplete cell populations other than monocytes and macrophages, we repeated our experiment by administering F4/80 neutralizing antibody, an epitope more selective for macrophages. Mice treated with F4/80 neutralizing antibody compared isotype control antibody exhibited less weight gain, lower RV systolic pressure, lower RV end-diastolic pressure, lower Fulton index, and less muscularization of lung vessels, similar to findings after clodronate treatment (Suppl Fig. 8).

IL1β Contributes to Pulmonary Vascular Remodeling in HFpEF

We finally sought to test the hypothesis that IL1β promotes pulmonary vascular remodeling in response to L-NAME/HFD treatment. To mimic a treatment or reversal model that would be more clinically relevant, we first treated mice with L-NAME and HFD for 3 weeks, followed by continuation of L-NAME/HFD with concomitant administration of either an IL1β neutralizing antibody or an isotype control (Fig 7A). Inhibition of IL1β decreased IL1β levels in the lung by ELISA (Fig 7B), decreased RV systolic pressure (Fig 7C), and decreased RV mass as compared to LV and septal mass (Fig 7D). No changes in RV end-diastolic pressure or weight gain were observed (Fig 7E,F). Histologically, IL1β depletion

resulted in a decrease in small vessel muscularization (Fig 7G). Given our previous data identifying myeloid cells as the primary source of IL1β, these findings now demonstrate that myeloid-derived IL1β is a key mediator of PH-HFpEF.

DISCUSSION

Pulmonary vascular remodeling is a highly morbid condition that commonly occurs in HFpEF, but pathways that drive remodeling during HFpEF are poorly understood. The present study demonstrates that a widely accepted multi-hit model of metabolically driven HFpEF, induced by the administration of L-NAME and a HFD, also exhibits features of pulmonary vascular remodeling and PH, comorbidities often found in patients with HFpEF.[2] Using a discovery based approach,, we report that circulating monocyte/macrophage populations and IL1β contribute to pathologic pulmonary vascular remodeling in HFpEF, findings validated by a second HFpEF animal model as well as human lung and plasma samples.

Heart failure is estimated to affect nearly 20% of the US population throughout their lifetime, approximately half of which constitutes HFpEF and carries up to a 75% 5-year mortality despite no current available therapies that improve mortality in this population.[18,19] The coexisting presence of PH, which variably occurs in up to 80% of patients with HFpEF,[20] is independently associated with a worse prognosis.[21] To date, however, strategies to prevent or reverse PH in HFpEF have been hampered by a limited understanding of the molecular mechanisms underlying pathologic pulmonary vascular remodeling, which has been identified as a key research priority for the study of HFpEF.[3,22]

Our study adds to the growing list of available models that approximate features of pathologic pulmonary vascular remodeling in HFpEF.[23–25] The L-NAME/HFD model has several distinct advantages in that it is technically straightforward to implement, replicates known deficits in nitric oxide and PKG signaling from human studies of HFpEF,[26,27] recapitulates many extra-cardiac features of HFpEF, including metabolic disease that is prominent in the human condition,[28] and is very amenable to further mechanistic studies.

Using a discovery-based approach, our study found inflammatory pathways to be altered in the remodeling lung of PH-HFpEF mice. Specifically, we identified monocyte/macrophage populations and IL1β as key mediators of pathologic pulmonary vascular remodeling. These findings were corroborated by human samples from patients with PH-HFpEF and, importantly, mirrored the results of clinical and pre-clinical studies that implicated inflammatory pathways in the pathogenesis of PH in HFpEF, including IL1β.[23,29] The role of IL1β in regulating endothelial cell permeability and lung injury is well established,[17,30] and activation of the NLRP3 inflammasome (upstream of IL1β expression and release) has been shown to regulate PH and RV failure in other forms of PH not related to heart failure as well.[31] Finally, studies have also found that macrophage-mediated IL1β partially regulates cardiac remodeling in the animal models of HFpEF.[32] Our study expands upon these initial findings by demonstrating that the extracardiac manifestation of pulmonary vascular remodeling is also partially regulated by monocyte/macrophage populations and IL1β. Our study showed that the cytokine profile of the lung differed from that of the

plasma in our animal model of HFpEF, however. These findings suggest that organ-specific inflammation in HFpEF may be modified, in part, by the microenvironment within specific organs, however further work is necessary to directly test this hypothesis.

There are limitations to our work. While our study focused on the role of monocyte/macrophages and IL1β in regulating pulmonary vascular remodeling in the L-NAME/HFD model of HFpEF, our findings also identify other inflammatory cell types and cytokines that are present within the lung. We cannot exclude the contribution of other cell types and cytokines to pulmonary vascular remodeling. Furthermore, while our plasma cytokine profile significantly differed from the lung cytokine profile, we cannot definitively exclude the possibility that extrapulmonary effects of monocyte/macrophage or IL1β depletion regulate pulmonary vascular remodeling through interorgan communication. Our studies demonstrated that other cell sources such as neutrophils also expressed IL1β and likely contributed to IL1β-mediated pulmonary vascular remodeling. While studies have shown that clodronate-mediated depletion of monocyte/macrophage populations in the lung can also reduce neutrophil recruitment and activation,[33] we cannot definitively rule out the contribution of neutrophil derived IL1β to pulmonary vascular remodeling in HFpEF. Additionally, while our findings implicate IL1β as an important target cytokine for the regulation of pulmonary vascular remodeling, future studies are necessary to definitively identify the primary mechanism by which IL1β may cause pulmonary vascular remodeling in HFpEF. Finally, our study focused on the combined administration of L-NAME and HFD to stimulate the HFpEF phenotype in mice based on previous studies that demonstrated that neither stimulus alone was sufficient to model HFpEF,[5] but our current study cannot definitively distinguish the individual contribution L-NAME or HFD to our findings.

In summary, our study demonstrates that the L-NAME/HFD model of HFpEF recapitulates features of pulmonary vascular remodeling observed in HFpEF patients. Moreover, it identifies monocyte/macrophage populations and IL1β as key mediators of pathologic pulmonary vascular remodeling in HFpEF. These findings not only provide novel insight into the elusive pathophysiology of pulmonary vascular remodeling in heart failure, but also raise important questions regarding the interplay between metabolic syndrome-driven cardiac disease and pulmonary vascular inflammation. With the growth of anti-inflammatory therapies in the treatment of cardiovascular disorders such as IL-1β targeting therapies, and recent insights into the immunomodulatory properties of more contemporary anti-diabetes therapies such as GLP-1 agonists and SGLT2 inhibitors, the PH-HFpEF model induced by L-NAME+HFD diet treatment in mice may serve as an important vehicle for not only identifying relevant pathophysiologic mechanisms in PH-HFpEF but also testing promising potential therapies.

Supplementary Material

Refer to Web version on PubMed Central for supplementary material.

Funding sources

This work was supported by NHLBI 1K08HL153956 (VA); Veterans Affairs 1IK2BX005828 (VA); National Center for Advancing Translational Sciences (NCATS) Clinical Translational Science Award (CTSA) Program,

Award Number 5UL1TR002243-03, project VR52924 (VA); Team Phenomenal Hope Foundation (VA); P01 HL108800 (ARH); K24 HL155891 (ARH); Gilead Sciences IN-US-300-0155 (Gilead Sciences) (KM); R01HL145372 (JAK); R01HL153246 (JAK); Vanderbilt Faculty Research Scholars Award (JJG).

ABBREVIATIONS AND NON-STANDARD ACRONYMS

ELISA	enzyme linked immunosorbent assay
HFpEF	Heart Failure with Preserved Ejection Fraction
HFD	high fat diet
IL1β	interleukin 1 beta
L-NAME	N(gamma)-nitro-L-arginine methyl ester
PAH	pulmonary arterial hypertension
PH	Pulmonary Hypertension
PH-HFpEF	pulmonary hypertension and heart failure with preserved ejection fraction
RNA	ribonucleic acid
RV	right ventricle

REFERENCES

1. Ibe T, Wada H, Sakakura K, Ugata Y, Maki H, Yamamoto K, Seguchi M, Taniguchi Y, Jinnouchi H, Momomura SI, et al. Combined pre- and post-capillary pulmonary hypertension: The clinical implications for patients with heart failure. PLoS One. 2021;16:e0247987. doi: 10.1371/journal.pone.0247987 [PubMed: 33651852]
2. Fayyaz AU, Edwards WD, Maleszewski JJ, Konik EA, DuBrock HM, Borlaug BA, Frantz RP, Jenkins SM, Redfield MM. Global Pulmonary Vascular Remodeling in Pulmonary Hypertension Associated With Heart Failure and Preserved or Reduced Ejection Fraction. Circulation. 2018;137:1796–1810. doi: 10.1161/circulationaha.117.031608 [PubMed: 29246894]
3. Boucherat O, Agrawal V, Lawrie A, Bonnet S. The Latest in Animal Models of Pulmonary Hypertension and Right Ventricular Failure. Circ Res. 2022;130:1466–1486. doi: 10.1161/circresaha.121.319971 [PubMed: 35482834]
4. Brittain EL, Thenappan T, Huston JH, Agrawal V, Lai YC, Dixon D, Ryan JJ, Lewis EF, Redfield MM, Shah SJ, et al. Elucidating the Clinical Implications and Pathophysiology of Pulmonary Hypertension in Heart Failure With Preserved Ejection Fraction: A Call to Action: A Science Advisory From the American Heart Association. Circulation. 2022;146:e73–e88. doi: 10.1161/cir.0000000000001079 [PubMed: 35862198]
5. Schiattarella GG, Altamirano F, Tong D, French KM, Villalobos E, Kim SY, Luo X, Jiang N, May HI, Wang ZV, et al. Nitrosative stress drives heart failure with preserved ejection fraction. Nature. 2019;568:351–356. doi: 10.1038/s41586-019-1100-z [PubMed: 30971818]
6. Agrawal V, Fortune N, Yu S, Fuentes J, Shi F, Nichols D, Gleaves L, Poovey E, Wang TJ, Brittain EL, et al. Natriuretic peptide receptor C contributes to disproportionate right ventricular hypertrophy in a rodent model of obesity-induced heart failure with preserved ejection fraction with pulmonary hypertension. Pulm Circ. 2019;9:2045894019878599. doi: 10.1177/2045894019895452
7. Brittain E, Penner NL, West J, Hemnes A. Echocardiographic assessment of the right heart in mice. J Vis Exp. 2013. doi: 10.3791/50912

8. Meoli DF, Clark DE, Davogustto G, Su YR, Brittain EL, Hemnes AR, Monahan K. Biomarker-specific differences between transpulmonary and peripheral arterial-venous blood sampling in patients with pulmonary hypertension. Biomarkers. 2020;25:131–136. doi: 10.1080/1354750x.2019.1710256 [PubMed: 31903794]
9. Meoli DF, Su YR, Brittain EL, Robbins IM, Hemnes AR, Monahan K. The transpulmonary ratio of endothelin 1 is elevated in patients with preserved left ventricular ejection fraction and combined pre- and post-capillary pulmonary hypertension. Pulm Circ. 2018;8:2045893217745019. doi: 10.1177/2045893217745019 [PubMed: 29251543]
10. Fleming SJ, Chaffin MD, Arduini A, Akkad A-D, Banks E, Marioni JC, Philippakis AA, Ellinor PT, Babadi M. Unsupervised removal of systematic background noise from droplet-based single-cell experiments using CellBender. bioRxiv. 2022:791699. doi: 10.1101/791699
11. Hao Y, Hao S, Andersen-Nissen E, Mauck WM 3rd, Zheng S, Butler A, Lee MJ, Wilk AJ, Darby C, Zager M, et al. Integrated analysis of multimodal single-cell data. Cell. 2021;184:3573–3587.e3529. doi: 10.1016/j.cell.2021.04.048 [PubMed: 34062119]
12. Habermann AC, Gutierrez AJ, Bui LT, Yahn SL, Winters NI, Calvi CL, Peter L, Chung MI, Taylor CJ, Jetter C, et al. Single-cell RNA sequencing reveals profibrotic roles of distinct epithelial and mesenchymal lineages in pulmonary fibrosis. Sci Adv. 2020;6:eaba1972. doi: 10.1126/sciadv.aba1972
13. Negretti NM, Plosa EJ, Benjamin JT, Schuler BA, Habermann AC, Jetter CS, Gulleman P, Bunn C, Hackett AN, Ransom M, et al. A single-cell atlas of mouse lung development. Development. 2021;148. doi: 10.1242/dev.199512
14. Natri HM, Azodi CBD, Peter L, Taylor CJ, Chugh S, Kendle R, Chung M-i, Flaherty DK, Matlock BK, Calvi CL, et al. Cell type-specific and disease-associated eQTL in the human lung. bioRxiv. 2023:2023.2003.2017.533161. doi: 10.1101/2023.03.17.533161
15. Guo M, Morley MP, Wu Y, Du Y, Zhao S, Wagner A, Kouril M, Jin K, Gaddis N, Kitzmiller JA, et al. Guided construction of single cell reference for human and mouse lung. bioRxiv. 2022:2022.2005.2018.491687. doi: 10.1101/2022.05.18.491687
16. Consortium TM. Single-cell transcriptomics of 20 mouse organs creates a Tabula Muris. Nature. 2018;562:367–372. doi: 10.1038/s41586-018-0590-4 [PubMed: 30283141]
17. Puhlmann M, Weinreich DM, Farma JM, Carroll NM, Turner EM, Alexander HR Jr. Interleukin-1beta induced vascular permeability is dependent on induction of endothelial tissue factor (TF) activity. J Transl Med. 2005;3:37. doi: 10.1186/1479-5876-3-37 [PubMed: 16197553]
18. Parikh KS, Sharma K, Fiuzat M, Surks HK, George JT, Honarpour N, Depre C, Desvigne-Nickens P, Nkulikiyinka R, Lewis GD, et al. Heart Failure With Preserved Ejection Fraction Expert Panel Report: Current Controversies and Implications for Clinical Trials. JACC Heart Fail. 2018;6:619–632. doi: 10.1016/j.jchf.2018.06.008
19. Shah KS, Xu H, Matsouaka RA, Bhatt DL, Heidenreich PA, Hernandez AF, Devore AD, Yancy CW, Fonarow GC. Heart Failure With Preserved, Borderline, and Reduced Ejection Fraction: 5-Year Outcomes. J Am Coll Cardiol. 2017;70:2476–2486. doi: 10.1016/j.jacc.2017.08.074 [PubMed: 29141781]
20. Lam CS, Roger VL, Rodeheffer RJ, Borlaug BA, Enders FT, Redfield MM. Pulmonary hypertension in heart failure with preserved ejection fraction: a community-based study. J Am Coll Cardiol. 2009;53:1119–1126. doi: 10.1016/j.jacc.2008.11.051 [PubMed: 19324256]
21. Dzudie A, Kengne AP, Thienemann F, Sliwa K. Predictors of hospitalisations for heart failure and mortality in patients with pulmonary hypertension associated with left heart disease: a systematic review. BMJ Open. 2014;4:e004843. doi: 10.1136/bmjopen-2014-004843
22. Shah SJ, Borlaug BA, Kitzman DW, McCulloch AD, Blaxall BC, Agarwal R, Chirinos JA, Collins S, Deo RC, Gladwin MT, et al. Research Priorities for Heart Failure With Preserved Ejection Fraction: National Heart, Lung, and Blood Institute Working Group Summary. Circulation. 2020;141:1001–1026. doi: 10.1161/circulationaha.119.041886 [PubMed: 32202936]
23. Ranchoux B, Nadeau V, Bourgeois A, Provencher S, Tremblay É, Omura J, Coté N, Abu-Alhayja'a R, Dumais V, Nachbar RT, et al. Metabolic Syndrome Exacerbates Pulmonary Hypertension due to Left Heart Disease. Circ Res. 2019;125:449–466. doi: 10.1161/circresaha.118.314555 [PubMed: 31154939]

24. Fayyaz AU, Sabbah MS, Dasari S, Griffiths LG, DuBrock HM, Wang Y, Charlesworth MC, Borlaug BA, Jenkins SM, Edwards WD, et al. Histologic and proteomic remodeling of the pulmonary veins and arteries in a porcine model of chronic pulmonary venous hypertension. Cardiovasc Res. 2023;119:268–282. doi: 10.1093/cvr/cvac005 [PubMed: 35022664]
25. Lai YC, Tabima DM, Dube JJ, Hughan KS, Vanderpool RR, Goncharov DA, St Croix CM, Garcia-Ocaña A, Goncharova EA, Tofovic SP, et al. SIRT3-AMP-Activated Protein Kinase Activation by Nitrite and Metformin Improves Hyperglycemia and Normalizes Pulmonary Hypertension Associated With Heart Failure With Preserved Ejection Fraction. Circulation. 2016;133:717–731. doi: 10.1161/circulationaha.115.018935 [PubMed: 26813102]
26. van Heerebeek L, Hamdani N, Falcão-Pires I, Leite-Moreira AF, Begieneman MP, Bronzwaer JG, van der Velden J, Stienen GJ, Laarman GJ, Somsen A, et al. Low myocardial protein kinase G activity in heart failure with preserved ejection fraction. Circulation. 2012;126:830–839. doi: 10.1161/circulationaha.111.076075 [PubMed: 22806632]
27. Lee DI, Zhu G, Sasaki T, Cho GS, Hamdani N, Holewinski R, Jo SH, Danner T, Zhang M, Rainer PP, et al. Phosphodiesterase 9A controls nitric-oxide-independent cGMP and hypertrophic heart disease. Nature. 2015;519:472–476. doi: 10.1038/nature14332 [PubMed: 25799991]
28. Rao VN, Fudim M, Mentz RJ, Michos ED, Felker GM. Regional adiposity and heart failure with preserved ejection fraction. Eur J Heart Fail. 2020;22:1540–1550. doi: 10.1002/ejhf.1956 [PubMed: 32619081]
29. Sabbah MS, Fayyaz AU, de Denus S, Felker GM, Borlaug BA, Dasari S, Carter RE, Redfield MM. Obese-Inflammatory Phenotypes in Heart Failure With Preserved Ejection Fraction. Circ Heart Fail. 2020;13:e006414. doi: 10.1161/circheartfailure.119.006414 [PubMed: 32809874]
30. Du L, Dong F, Guo L, Hou Y, Yi F, Liu J, Xu D. Interleukin-1β increases permeability and upregulates the expression of vascular endothelial-cadherin in human renal glomerular endothelial cells. Mol Med Rep. 2015;11:3708–3714. doi: 10.3892/mmr.2015.3172 [PubMed: 25572875]
31. Al-Qazazi R, Lima PDA, Prisco SZ, Potus F, Dasgupta A, Chen KH, Tian L, Bentley RET, Mewburn J, Martin AY, et al. Macrophage-NLRP3 Activation Promotes Right Ventricle Failure in Pulmonary Arterial Hypertension. Am J Respir Crit Care Med. 2022;206:608–624. doi: 10.1164/rccm.202110-2274OC [PubMed: 35699679]
32. Liu H, Huang Y, Zhao Y, Kang GJ, Feng F, Wang X, Liu M, Shi G, Revelo X, Bernlohr D, et al. Inflammatory Macrophage Interleukin-1β Mediates High-Fat Diet-Induced Heart Failure With Preserved Ejection Fraction. JACC Basic Transl Sci. 2023;8:174–185. doi: 10.1016/j.jacbts.2022.08.003 [PubMed: 36908663]
33. Beck-Schimmer B, Schwendener R, Pasch T, Reyes L, Booy C, Schimmer RC. Alveolar macrophages regulate neutrophil recruitment in endotoxin-induced lung injury. Respir Res. 2005;6:61. doi: 10.1186/1465-9921-6-61 [PubMed: 15972102]

NOVELTY AND SIGNIFICANCE

WHAT IS KNOWN?

- Pulmonary hypertension (PH) due to heart failure is the most common cause of PH worldwide, but unlike other forms of PH, has no dedicated therapies that reduce mortality.
- Limited animal models, and specifically murine models, of PH due to heart failure exist to better understand pathogenic mechanisms underlying PH in heart failure.

WHAT NEW INFORMATION DOES THIS ARTICLE CONTRIBUTE?

- This study presents a new murine model of PH due to heart failure with preserved ejection fraction (HFpEF) and identifies myeloid-derived IL1β as a significant contributor to pathologic pulmonary vascular remodeling in HFpEF.
- Findings were replicated in a second model of HFpEF, the db/db mouse model, in human lung samples from patients with PH-HFpEF who underwent autopsy, and in plasma from patients with PH-HFpEF undergoing catheterization.

The findings suggest that targeted therapies for IL1β may be efficacious in preventing and reversing PH due to HFpEF.

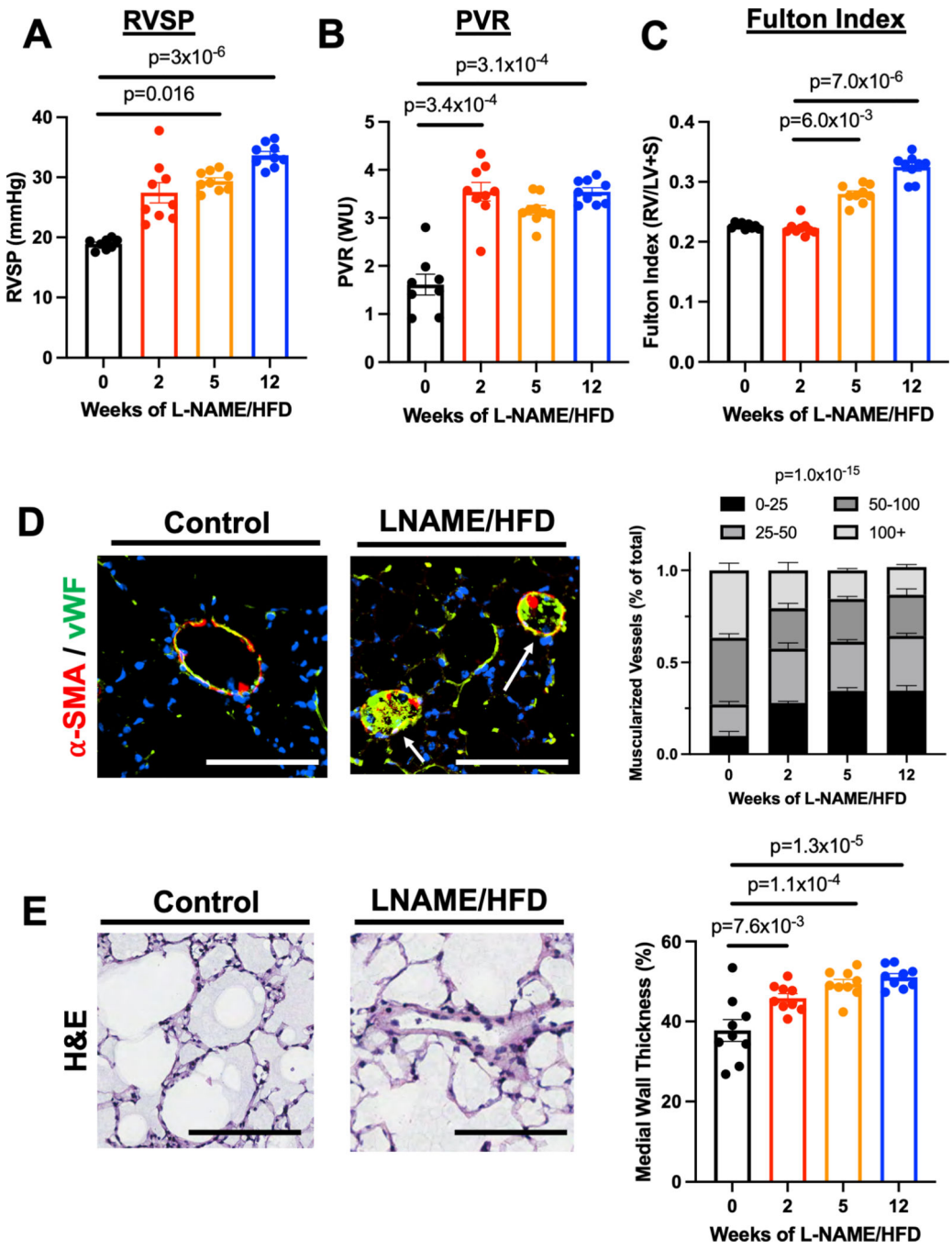

Figure 1.

L-NAME and high fat diet treatment in mice causes (A) increased right ventricular systolic pressure, (B) increased pulmonary vascular resistance, (C) increased right ventricular mass relative to left ventricular and septal mass, (D) muscularization of small pulmonary vessels (< 50 μm) in lungs (bars = 50 μm), and (E) increased medial wall thickness of pulmonary vessels in lungs. ** $p < 0.05$, ** $p < 0.01$, *** $p < 0.001$, **** $p < 0.0001$ compared to baseline or control. n=9 for all groups (5 males, 4 females).*

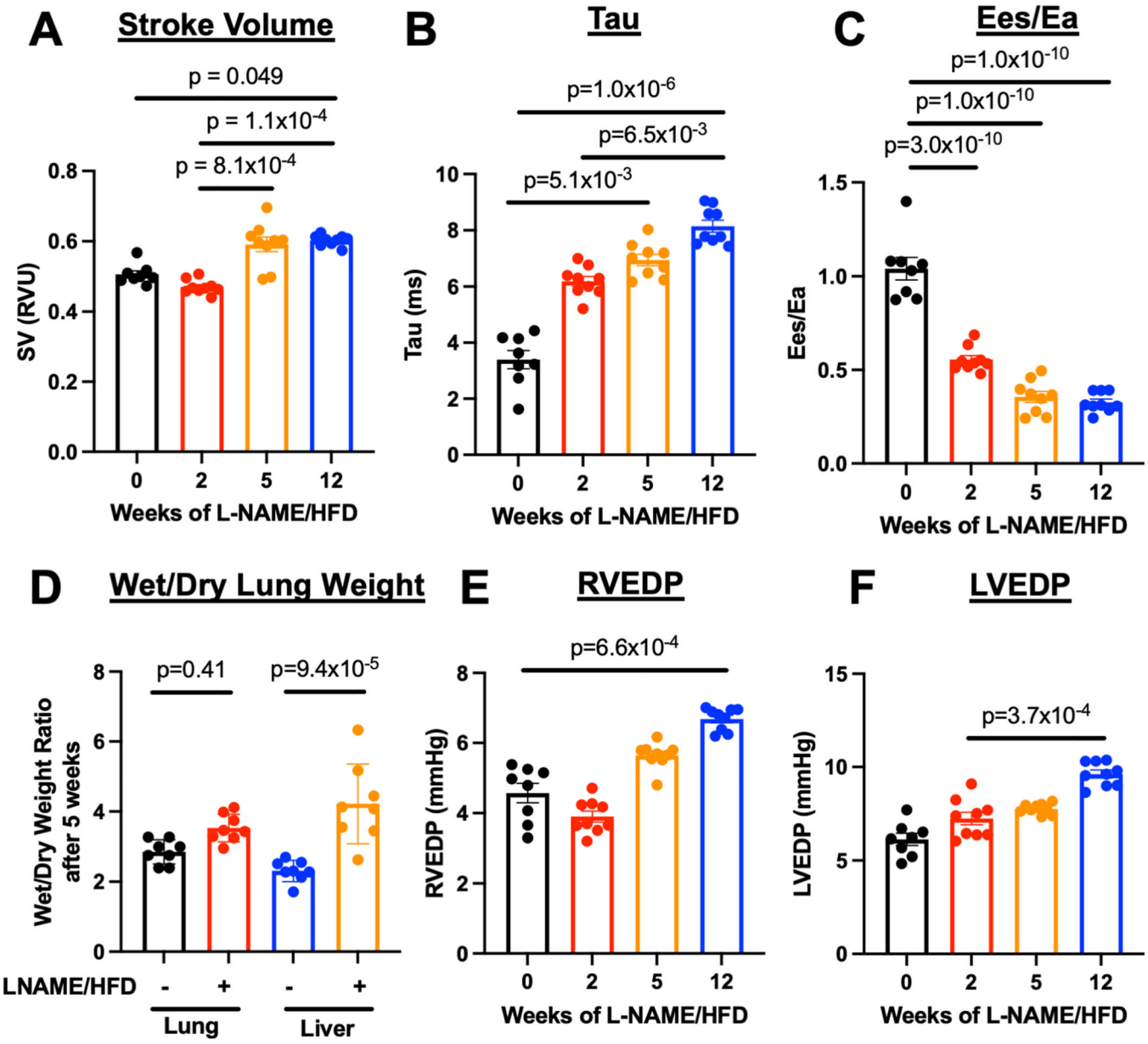

Figure 2.

L-NAME and high fat diet treatment in mice (A) preserves stroke volume, (B) increased diastolic stiffness of the right ventricle as measured by the relaxation constant (τ), (C) decreased right ventricle-to-pulmonary artery coupling, (D) increased right heart congestion as measured by wet-to-dry liver mass, (E) increased right ventricular end-diastolic pressure, and (F) increased left ventricular end-diastolic pressure. ** p < 0.05, ** p < 0.01, *** p < 0.001, **** p < 0.0001 compared to baseline or control. n=9 for all groups (5 males, 4 females).*

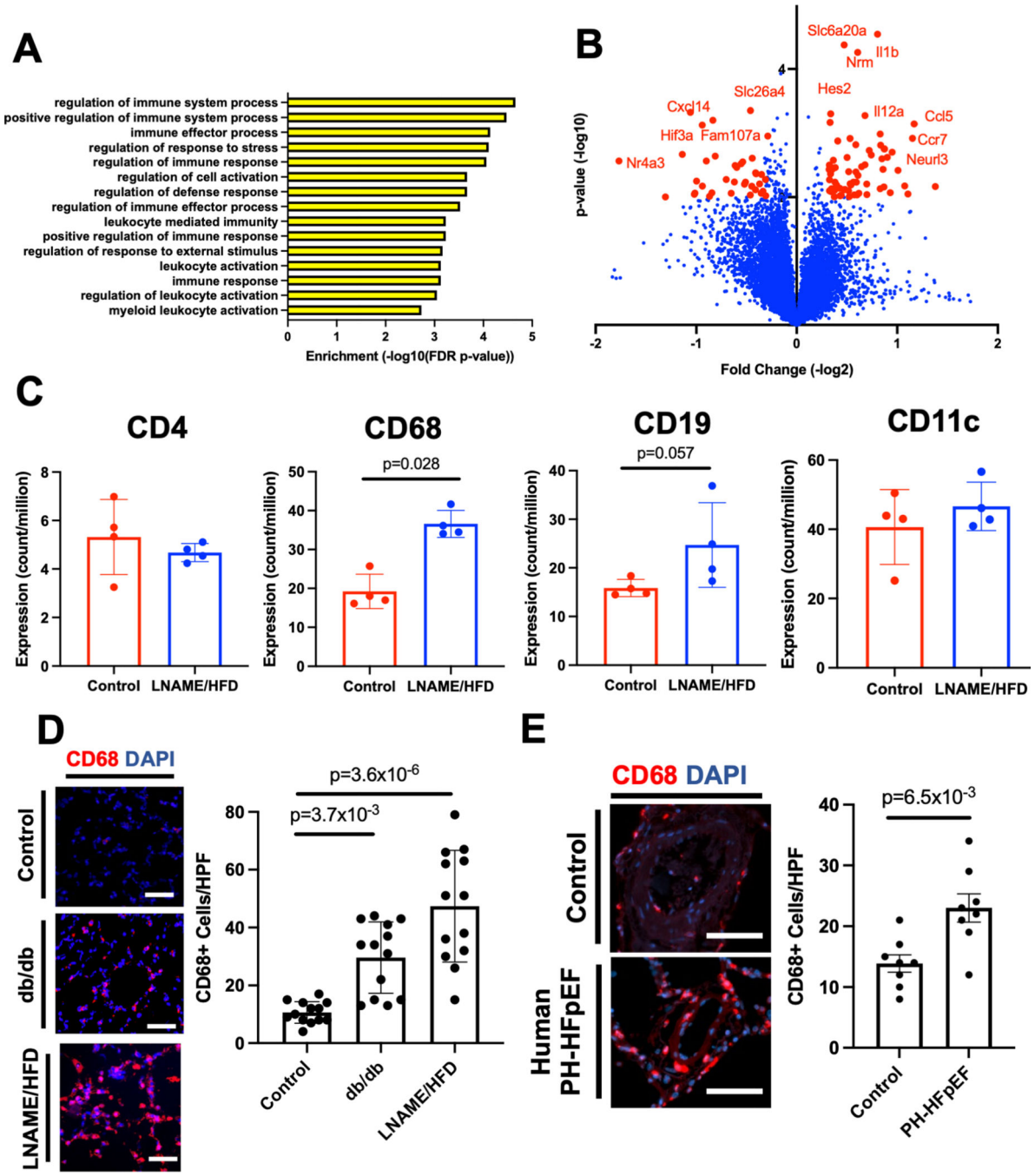

Figure 3.

Bulk RNA sequencing of the whole lung in L-NAME and high fat diet (HFD) treated lungs compared to control identify that: (A) inflammatory gene ontologies are the top 15 most over-represented ontologies in the L-NAME/HFD treated lung, (B) transcript expression of cytokines represent the most differentially expressed transcripts, (C) transcript expression of macrophage marker CD68 is increased in the L-NAME/HFD treated lungs, (D) an increase in CD68+ cells in two animal models of heart failure with preserved ejection fraction (bars = 50 μm), and (E) an increase in CD68+ cells in the lungs of patients with PH-HFpEF who

underwent autopsy at death (n=8 per group, bars = 100 μm). ** $p < 0.05$, ** $p < 0.01$, *** $p < 0.001$, **** $p < 0.0001$ compared to baseline or control. RNA sequencing studies were conducted once from 4 separate animals. Immunostaining for CD68 in mouse models were performed from 12 mice per group (equal numbers male and female), and lung sections from 8 patients in each group with either PH-HFpEF or control.*

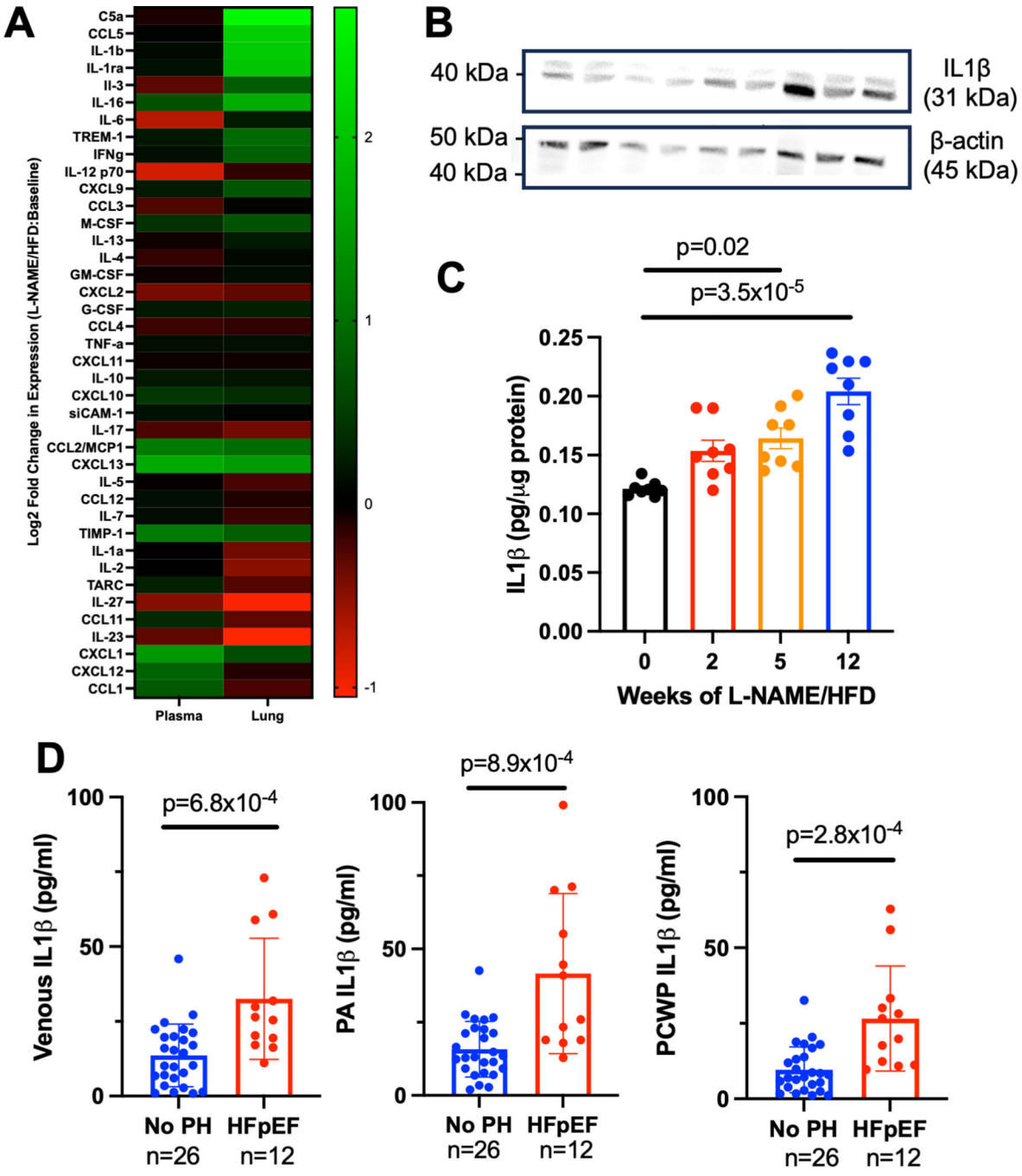

Figure 4.

(A) Cytokine array in lungs and plasma of mice treated with L-NAME and high fat diet compared to control demonstrate lung-specific increases in cytokines and chemokines. (B) Western blot for IL1β confirms an increase in expression of mice treated with L-NAME and high fat diet (n=3 per group). (C) ELISA for IL1β demonstrate an increase in expression in L-NAME/HFD treated mice (n=6–7 per group). (D) IL1β levels by ELISA are increased in the venous, pulmonary artery, and pulmonary capillary wedge blood of patients with HFpEF compared to control patients without pulmonary hypertension. *$p < 0.05$, **$p < 0.01$, ***

*$p < 0.001$, **** $p < 0.0001$ compared to baseline or control. Cytokine array was performed once as an exploratory technique from pooled samples from n=5 control mice and n=5 mice treated with L-NAME/HFD.*

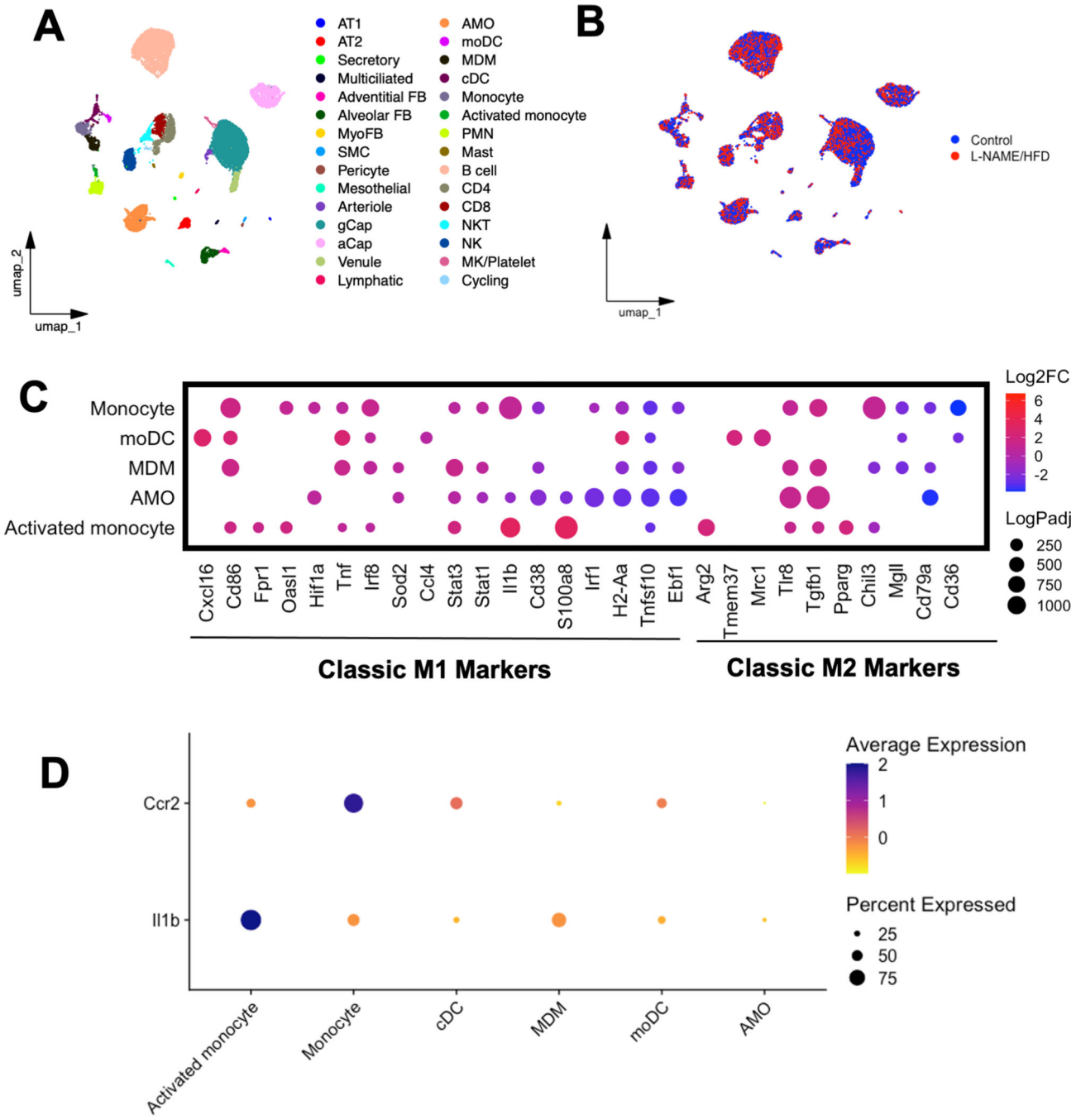

Figure 5.

UMAP embedding of single cell RNA sequencing of lungs from mice treated with either L-NAME and high fat diet or control annotated by (A) cell type and (B) treatment group. (C) Transcript expression of classic M1 and M2 macrophage markers in various monocyte/macrophage populations in the lung. (D) Expression of Ccr2, a marker of circulating myeloid cells, and Il1β in various cell populations in the lung. *Experiments were conducted once from n=4 control mice and n=4 L-NAME/HFD treated mice.*

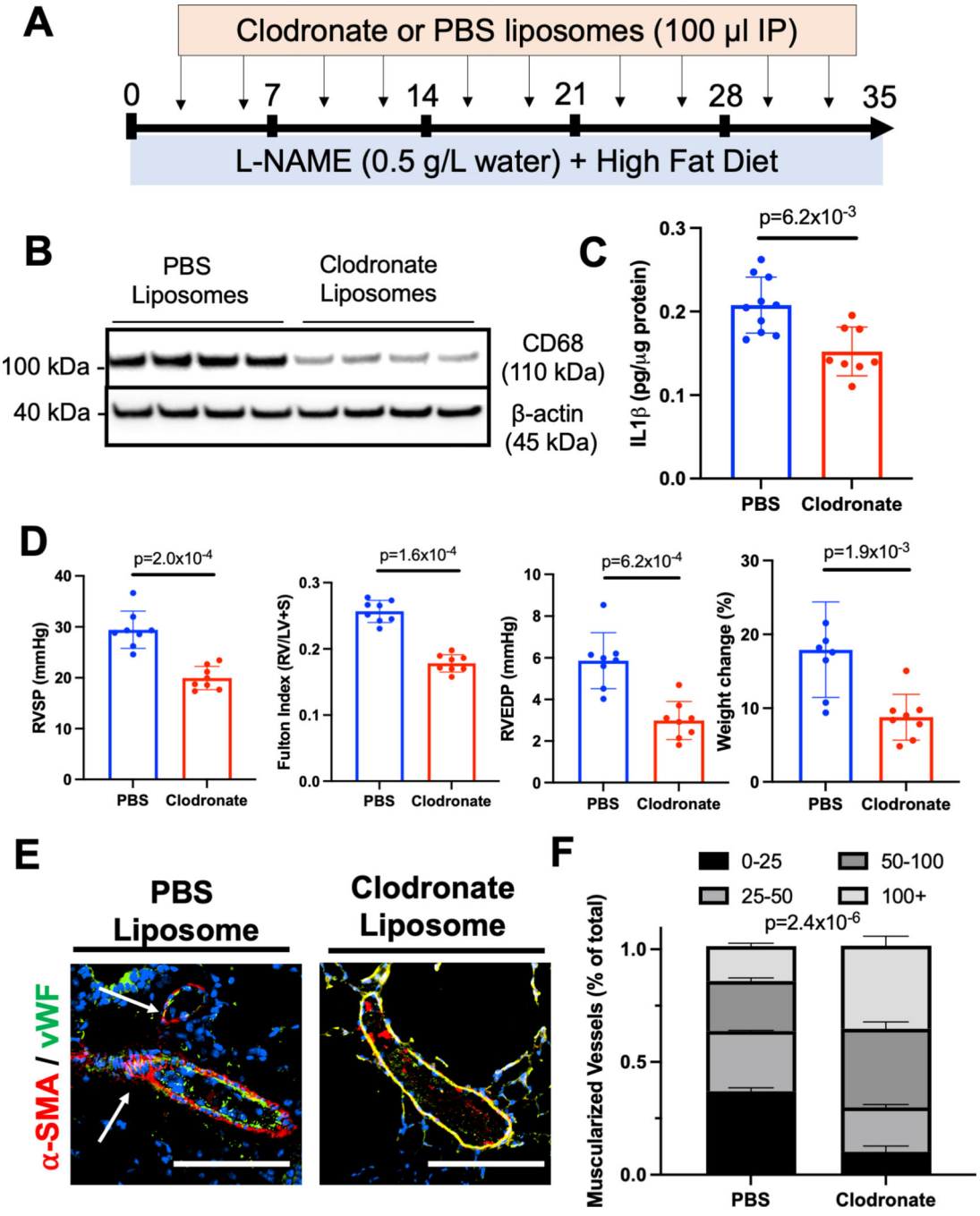

Figure 6.

(A) Schematic depiction of clodronate-mediated monocyte/macrophage depletion studies. (B) CD68 expression by Western blot in the lung after clodronate or PBS liposome treatment. (C) IL1β levels by ELISA in the whole lung after clodronate or PBS liposome treatment. (D) Right ventricular systolic pressure, right ventricular mass relative to left ventricular and septal mass, right ventricular end-diastolic pressure, and weight change in mice after clodronate vs PBS liposome treatment. (E) Muscularization of small vessels in the lungs decrease after clodronate treatment in L-NAME and high fat diet treated mice (bars

= 50 μm) . ** $p < 0.05$, ** $p < 0.01$, *** $p < 0.001$, **** $p < 0.0001$ compared to baseline or control. n=8 mice were used in each group for all studies except for IL1β cytokine measurements where n=10 PBS injected mice were used. .*

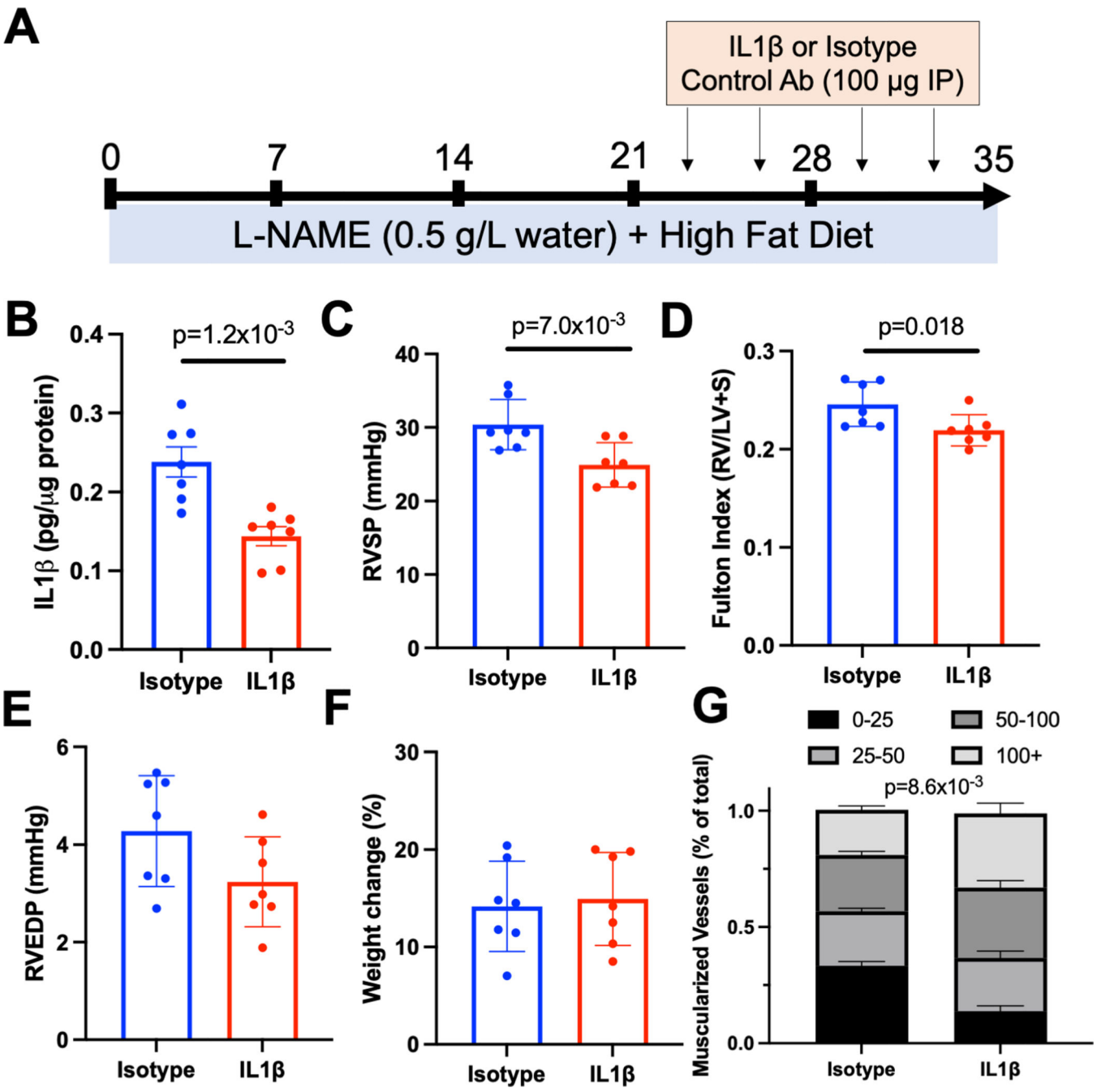

Figure 7.

(A) Schematic depiction of IL1β antibody mediated depletion studies. (B) Il1β levels by ELISA, (C) right ventricular systolic pressure, (C) right ventricular end-diastolic pressure, (D) weight change, and (E) muscularization of vessels in the lung after treatment with IL1β specific or isotype control antibody in mice treated with L-NAME and high fat diet. ** p < 0.05, ** p < 0.01, *** p < 0.001, **** p < 0.0001 compared to baseline or control. n=7 per group (4 females, 3 males).*